

Article

Integration of Remote Sensing Techniques for Intensity Zonation within a Landslide Area: A Case Study in the Northern Apennines, Italy

Veronica Tofani *, Chiara Del Ventisette, Sandro Moretti and Nicola Casagli

Department of Earth Sciences, University of Firenze, Via La Pira 4, I-50121 Firenze, Italy;

E-Mails: chiara.delventisette@unifi.it (C.D.V.); sandro.moretti@unifi.it (S.M.);

nicola.casagli@unifi.it (N.C.)

* Author to whom correspondence should be addressed; E-Mail: veronica.tofani@unifi.it;
Tel.: +39-055-275-7450

Received: 21 November 2013; in revised form: 30 December 2013 / Accepted: 31 December 2013 /

Published: 23 January 2014

Abstract: This paper describes the application of remote sensing techniques, based on SAR interferometry for the intensity zonation of the landslide affecting the Castagnola village (Northern Apennines of Liguria region, Italy). The study of the instability conditions of the landslide started in 2001 with the installation of conventional monitoring systems, such as inclinometers and crackmeters, ranging in time from April 2001 to April 2002, which allowed to define the deformation rates of the landslide and to locate the actual landslide sliding surface, as well as to record the intensity of the damages and cracks affecting the buildings located within the landslide perimeter. In order to investigate the past long-term evolution of the ground movements a PSI (Persistent Scatterers Interferometry) analysis has been performed making use of a set of ERS1/ERS2 images acquired in 1992–2001 period. The outcome of the PSI analysis has allowed to confirm the landslide extension as mapped within the official landslide inventory map as well as to reconstruct the past line-of-sight average velocities of the landslide and the time-series deformations. Following the high velocities detected by the PSI, and the extensive damages surveyed in the buildings of the village, the Ground-Based Interferometric Synthetic Aperture Radar (GBInSAR) system has been installed. The GBInSAR monitoring system has been equipped during October 2008 and three distinct campaigns have been carried out from October 2008 until March 2009. The interpretation of the data has allowed deriving a multi-temporal deformation map of the landslide, showing the up-to-date displacement field and the average landslide velocity. A new landslide boundary has been defined and

two landslide sectors characterized by different displacement rates have been identified.

Keywords: landslide; remote sensing; SAR interferometry; intensity assessment; Northern Apennines

1. Introduction

Many urban areas in Italy are located within landslide areas. In order to take decisions about future land planning and development and possible risk management strategies a detailed landslide hazard zonation has to be carried out. A correct and sound hazard zonation should include also the classification of landslide intensity. Landslide intensity as a set of spatially distributed parameters describing the destructiveness of the landslide was defined in [1]. Hungr [1] argued that the maximum movement velocity is the most important intensity parameter and defined a scale of destructiveness based on the velocity, which has been later modified by [2,3]. Other intensity parameters include total displacement, differential displacement, depth of the sliding surface, depth of the deposited mass, and depth of erosion.

Intensity is a measure of the damage capability of the landslide and the likelihood of damage to structures and the potentials for life-loss vary because of this [4].

In slow-moving landslides, people are not usually endangered, while damages to buildings and infrastructures might be high. On the contrary, rapid movements of small and large masses may have catastrophic consequences for both people and structures [4]. In some cases, the same landslide may result in different values of intensity along the path. For the above reasons, the definition of landslide intensity in zoning study is fundamental.

Landslide velocity, as well as total or differential displacements, can be measured by means of monitoring techniques. Generally, the conventional monitoring techniques—both geotechnical (extensometers, inclinometers, distometers, piezometers, *etc.*) and topographic (manual triangulation, total station, and GPS measurements)—provide accurate information on a selected number of points on the slopes affected by the instability phenomena. Very often, single-point data cannot be considered representative of the behavior of the whole landslide mass. Extensive conventional monitoring networks are usually installed on landslides to get rid of such spatial limiting characteristics, but, however, cannot be employed on landslide sectors which are at high risk or not accessible.

Remote sensing monitoring systems, based on radar techniques (Persistent Scatterers Interferometry—PSI and Ground-Based Interferometric Synthetic Aperture Radar—GBInSAR) can overcome most of these limitations. Radar sensors can operate over wide areas in almost any weather condition, continuously over a long time, providing real-time widespread information with millimetric accuracy without the need of accessing to the study area.

Space-borne differential SAR interferometry (DInSAR) techniques have shown their capability to provide wide area coverage and, under suitable conditions, spatially dense information on slow ground surface deformations [5]. A remarkable improvement is given by the DInSAR methods that make use of large sets of SAR images acquired over the same area. These techniques, called Advanced DInSAR (A-DInSAR), represent an outstanding advance with respect to the standard ones and overcome some limiting factors of conventional DInSAR, such as temporal and geometric decorrelation of reflectivity

and atmospheric disturbance [5,6]. Several A-DInSAR approaches have been proposed after the publication of the Permanent Scatterers Technique (PS-InSARTM) by [7]. Generally, the term Persistent Scatterers Interferometry (PSI) is employed to indicate all the multi-temporal techniques. PSI techniques have been applied to monitor landslides [8–11]. In particular, the availability of huge historical SAR archives confers to PSI the ability to measure and monitor “past deformation phenomena” [12]. Furthermore, the access to archived SAR data is useful to study temporal variations of motion that enable assessing slope stability, complementary to other information [13].

Ground-based SAR interferometry (GBInSAR) has been extensively used for spatial displacement monitoring of landslides [14–17].

The base principles of the ground-based SAR are the same of a satellite sensor, but, instead of along the orbit, the along track aperture is synthesized by moving the radar head along a short rail (2–3 m). Using this configuration, it is possible to produce a large number of images in a very short time (hours) with the same viewing angle, retrieving the ground deformations that occurred over the elapsed time with a zero baseline configuration. The resolution cell size of the SAR images in range and cross range directions is a function of the: (1) frequency bandwidth, (2) synthetic aperture length, and (3) distance of the observed area.

The capability to provide millimetric accurate displacements over areas up to a few square kilometers wide, combined with the capacity to monitor even rapid and slow movements, are the main reasons that have contributed to the use of the GBInSAR interferometry in landslide monitoring [18–20]. Moreover, the high temporal acquisition frequency and the simplicity and rapidity of GB-InSAR data analysis allows the technique to be used in near-real-time monitoring in order to predict the short-term evolution of movements and, consequently, to define the associated risk scenarios.

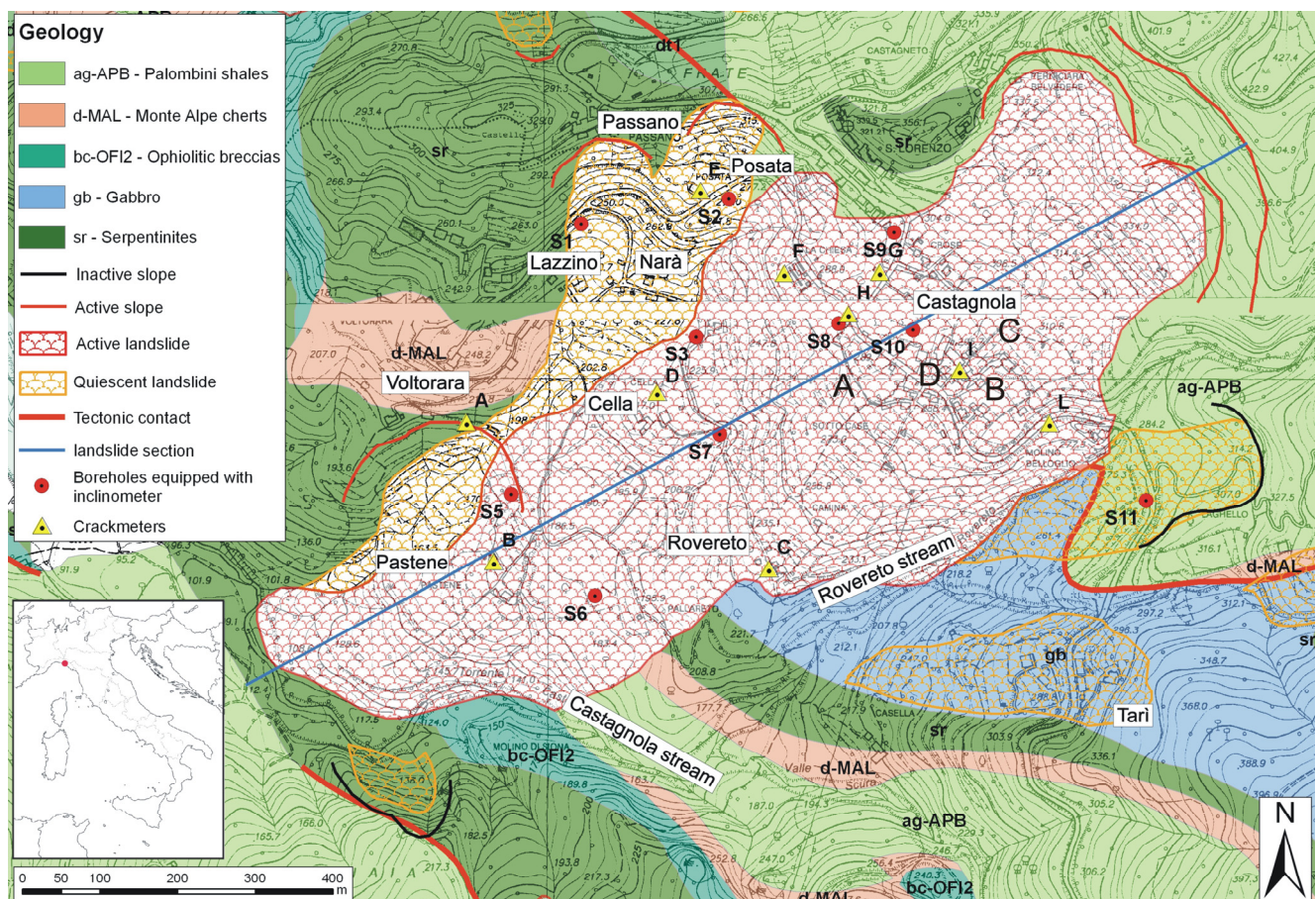
In this paper, following the geological and geomorphological description of the Castagnola landslide area and the conventional monitoring data available on the landslide, we investigate the application of both satellite and ground-based radar interferometry techniques for the intensity zonation of the landslide. The combination of PSI analysis performed on ERS1/ERS2 images acquired from 1992 to 2001, and the three GBInSAR survey campaigns carried out, discontinuously, from October 2008 to March 2009 has allowed to perform the landslide intensity zonation, distinguishing two landslide sectors characterized by different displacement rates and extending the landslide area. The combination of PSI and GB-InSAR has demonstrated as an efficient tool to retrieve past and real-time displacement data, which can support the definition of appropriate risk management strategies. This tool can be a sound base to develop new techniques for mapping and monitoring, not only landslides, but also other types of natural hazards.

2. Study Area and Landslide Investigation

The Castagnola landslide is a large landslide with an estimated volume of about 3 Mm³ located in the Northern Apennines, about 25 km to the N of La Spezia city and 2.5 km to the N-NE from the Eastern Ligurian coast (Figure 1). The landslide completely affects the Castagnola village where 200 people live permanently. The Ligurian Apennines, and their coastal area, are characterized by the extensive outcrops of rocks belonging to the Internal Ligurian Domain. These successions consist of a Jurassic-Paleocene oceanic sequence (“Supergruppo della Val di Vara”, [21]) with ophiolites. The ophiolites include a

gabbro and serpentinite basement and a portion of a volcano-sedimentary complex (ophiolitic breccias and basaltic lavas) covered by marine sediments (Monte Alpe Cherts, Calpionelle Limestone, and Palombini Shales) of Callovian-Santonian age (middle Jurassic—late Cretaceous, [22]).

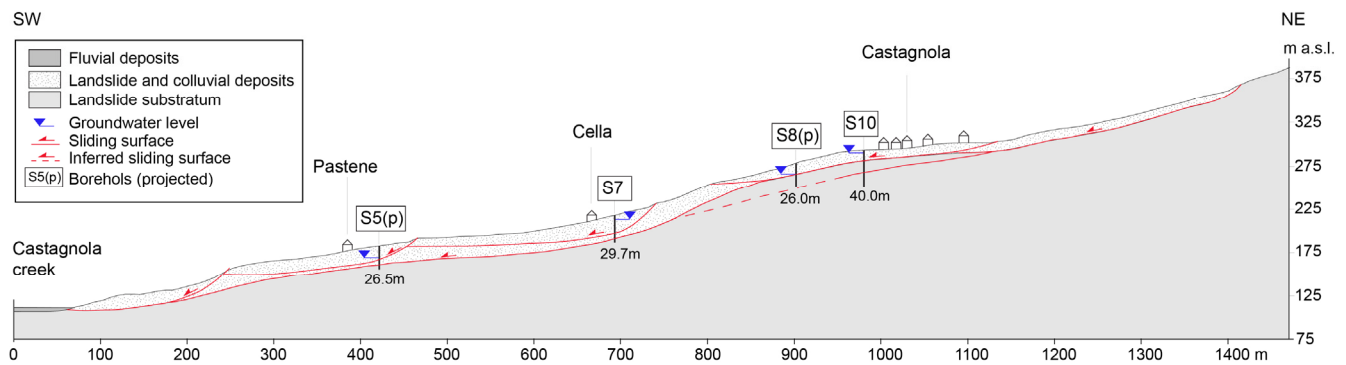
Figure 1. Geologic and geomorphologic map of Castagnola area with location of the *in-situ* instrumentation and landslide perimeter as mapped in the PAI (Hydrogeological Setting Plan).



The landslide affects the right flank of the Castagnola river valley, stretching from an altitude of about 350 m above sea level (a.s.l.) to the river bed (100 m a.s.l.) on a surface of 0.5 km² (1.3 km in length and 0.4 km wide) (Figure 1). The right flank of the valley is characterized by the presence of the reversed flank of an anticline verging towards NE where the overturned sequence Palombini Shales-Monte Alpe Cherts-Ophiolites crops out. The sequence slightly dips to SW (10°–20°) and the anticline core is limited by two major normal faults trending NW-SE.

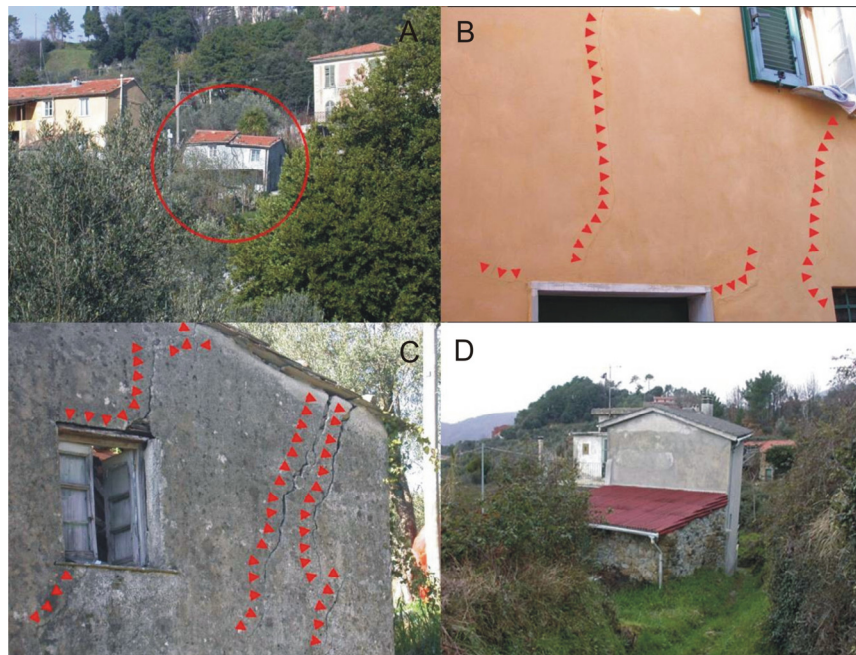
The landslide mass is bounded to the NE by a major scarp, while, on the SE it is limited by the deep incision of the Rovereto stream (Figure 1). The landslide mass extends to SW, reaching at the toe the right bank of the Castagnola river, which has been diverted by the progressive landslide accumulation.

The aerial photo interpretation, the morphological characteristics, and the geological arrangement of the area, highlight the presence of several rotational slips on which are superimposed minor shallow planar landslides (Figure 2). On surface, the landslide structure is, therefore, partially masked by the presence of discontinuous terraced alluvial deposits, colluvial and talus debris.

Figure 2. Landslide cross-section.

The geological model of the landslide was developed by integrating a new detailed geomorphological investigation with sub-surface data acquired from 10 boreholes, drilled between February and March 2001. The boreholes were subsequently equipped with inclinometers, which have allowed to actually locate the sliding surfaces of the phenomenon.

The landslide mass lithology is heterogeneous and predominantly consists of altered argillite with limestone and ophiolitic blocks interbedded with clays and silty-clays layers, with cobbles and gravels. The bedrock along the slope is constituted predominantly by Palombini Shales and to a lesser extent by Ophiolitic rocks (Serpentinites and Gabbro). The thickness of the altered and loose materials varies across the slope and progressively increases from the N area close to the head scarp (7–10 m) toward the toe of the landslide, reaching a thickness of 25 m on the borehole S7 (Figure 2).

Figure 3. Building damages caused by landslide activity. The (A–D) location of pictures is reported in Figure 1.

The landslide activity has disrupted the vegetation cover, which consists of sparse olive trees, rows of vines, and bushes, delineating a noticeably different pattern with respect to the surrounding stable area. The landslide interaction with the civil infrastructures is extensively observed: many buildings in Castagnola village and the surroundings show structural damages due to the landslide activity (Figure 3).

From April 2001 to April 2002, the deformational pattern of the Castagnola slope has been monitored by 10 inclinometers placed at different location on the landslide mass and 10 crackmeters (A–L) installed on damaged buildings, retaining walls, and roads (Figure 2).

The analysis of the inclinometric data highlights the presence of well-developed sliding surfaces at depths variable from 8 to 25 m on the S5, S7, S8, S9, S10, and S11 inclinometers located on the SE sector of the landslide. The highest annual displacements, respectively 175 and 163 mm, have been measured at the head of the S7 and S11 boreholes, although these inclinometers were sheared off at a depth of 20 m shortly after the installation, probably not capturing the total amount of the movement. In addition, the inclinometers, S8 and S10, which have recorded a total displacement of 33 and 82 mm, were sheared off respectively at a depth of 11 and 25 m. The azimuth recorded by the inclinometers is consistent with a SW landslide movement.

The other inclinometers installed in the N landslide sector (S1, S2, and S3) have shown slower deformation rates ($40\text{--}60\text{ mm}\cdot\text{yr}^{-1}$), not localized along well-defined levels (S1 and S2). Only on the inclinometric tube S3 is a very superficial shear surface, at a depth of 3 m, evident.

Regarding the crackmeters, the larger absolute displacements equal to 12 mm, from April 2001 to April 2002, has been recorded by F crackmeters, installed on a damaged wall of the Castagnola cemetery. The other instruments (in particular the A, C, and H crackmeters) have shown cumulated absolute displacements ranging from 5 to $10\text{ mm}\cdot\text{yr}^{-1}$.

3. Material and Methods

3.1. PSI

In order to investigate the past long-term evolution of the ground movements and to confirm the deformations rates measured by the conventional instrumentation, the PSI analysis has been performed with ERS1-ERS2 satellite images, in descending orbits, covering a period of 1992–2001.

SAR satellite imagery in C band (5.6 cm wavelength; frequency 5.3 GHz), acquired by the European Space Agency (ESA) satellites ERS1/2, was employed for the reconstruction of the history and spatial patterns of the Castagnola landslide. In particular, 76 ERS1/2 scenes, acquired along descending orbits from 24 April 1992 to 4 January 2001.

Rural areas seldom display a PS density comparable to that of urban areas and also, in this case, the distribution of PSI radar benchmarks is not homogeneous and is strongly influenced by the land cover. Most of the stable points are located in the Castagnola village. The slope exposure to the satellite line of sight has minimized the geometrical effects induced by the side-looking geometry of SAR system.

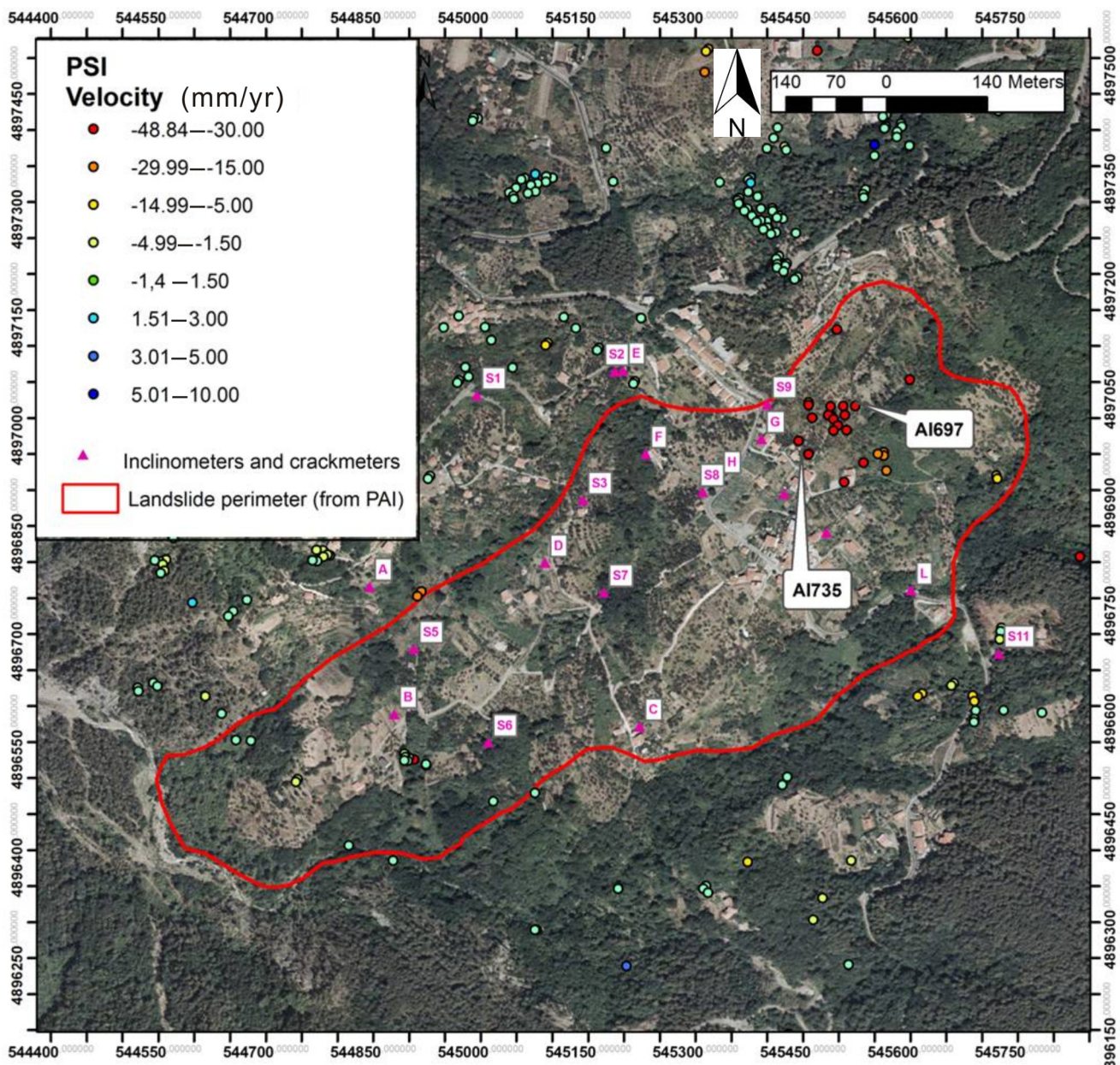
The distribution of radar persistent scatterers inside the active landslide, as mapped in the PAI (Hydrogeological Setting Plan), prepared by the La Spezia Province, is shown in Figure 4.

The color scale displays the values of superficial movements measured along the satellite line of sight (l.o.s.) expressed in $\text{mm}\cdot\text{yr}^{-1}$. The negative sign indicates a movement away from the SAR sensor, while positive values represent a movement towards the sensor.

The color scale indicates green PS points as stable. In descending orbit the gradation from yellow, orange, to red represents movement away from the sensor, while the gradation from light blue to dark

blue represents movements toward the sensor. Considering the slope aspect, the movements detected by the ERS satellite are consistent with a landslide moving to SW direction.

Figure 4. Distribution of radar benchmarks of PSI analysis within landslide perimeter (as reported in PAI map).



3.2. GB-InSAR

In 2008, a new advanced monitoring system of the landslide has been installed; the Ground-Based Interferometric Synthetic Aperture Radar (GBInSAR). The GBInSAR system installed in Castagnola belongs to the interferometer series called LISA (Linear Synthetic Aperture high-resolution radar), designed by JRC—Joint Research Center of the European Commission [23] and manufactured by Ellegi-LISALab Company.

GBInSAR system consists of a coherent microwave transceiver unit based on a precision network analyzer (PNA) working at Ku band, which generate a sweep of electromagnetic waves of proper

duration at different frequencies. The signal is then amplified and transmitted to the antennas. The synthetic aperture is realized by moving, via a linear positioner, a motorized sled hosting the radar head along a straight rail 2.7 m long (Figure 5). The main operational parameters adopted during the monitoring surveys are summarized in Table 1.

Figure 5. GBInSAR system used to monitor Castagnola landslide. The dotted line is the landslide perimeter.



Table 1. Summary of the main operational parameters of the radar measurement campaigns.

Operational Parameters	Values
Central Frequency	17.05 GHz
Bandwidth	100 MHz
Synthetic aperture	2.7 m
Minimum target distance	100 m
Maximum target distance	1,500 m
Range resolution	1.5 m
Cross-range resolution (at 100 m)	0.33 m
Cross-range resolution (at 800 m)	2.60 m
Cross-range resolution (at 1,500 m)	4.95 m
Polarisation	VV
Antenna gain	−20 dB

Using these acquisition parameters, the ground resolution in the range direction, which is a function of the employed bandwidth, was about 1.5 m, while the cross-range resolution (perpendicular to the range direction) was variable from 0.3 to 2.6 m, with a higher resolution for the landslide sector located close to the radar station.

GBInSAR system was installed on the roof of a municipal warehouse, at a mean distance of about 700 m from the landslide area (Figure 5). The first survey campaign was carried out over seven days, between 23 and 29 October 2008. Image acquisition was repeated at time intervals of about 10 min, acquiring a total of 907 radar images. During the second periodical check survey (from 10 to 18 February 2009) the GBInSAR system was installed again in the same position (zero baseline), acquiring a total of 1,231 images (Table 2).

Table 2. Ground-Based Interferometric Synthetic Aperture Radar (GB-InSAR) survey campaigns.

	Date	Duration (Days)	Number of Radar Images
First Campaign	23–29 October 2008	7	907
Second Campaign	10–18 February 2009	9	1,231
Third Campaign	23 February–13 March 2009	17	2,727

The daily analysis of the interferograms, obtained during the second campaign, has revealed conspicuous slope deformations with respect to the displacements observed during the first campaign. To follow the evolution of the landslide, and to avoid possible phase wrapping effect in the long-term interferograms, it has been decided to rapidly resume the radar survey in order to provide the local authorities with a near-real-time monitoring service. The last survey campaign was performed from 23 February to 13 March 2009, spanning 17 days and 22 h and acquiring 2,727 images.

During each campaign, GB-InSAR data were daily transferred via ftp to the processing and post-processing unit for the generations of both the interferograms and the cumulative displacement maps.

4. Results

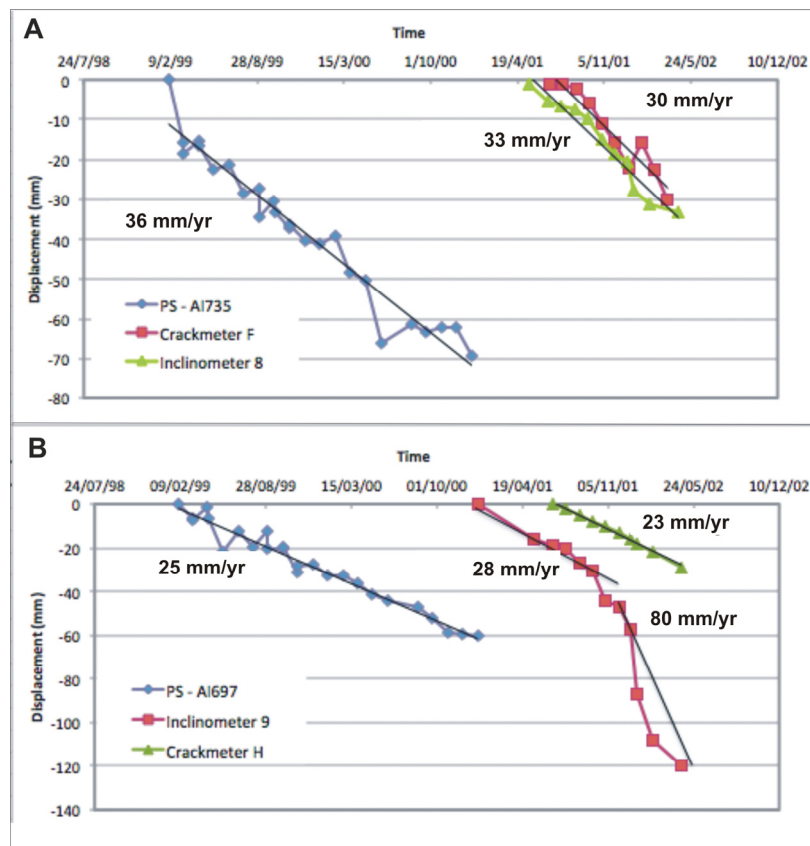
4.1. PSI

A total of 39 persistent scatterers are present inside the landslide perimeter, most of them in the up-slope portion of the landslide where the Castagnola village is located (Figure 4). The displacement velocities range between $0.9 \text{ mm}\cdot\text{yr}^{-1}$ to $42.2 \text{ mm}\cdot\text{yr}^{-1}$ as absolute value, with a mean velocity value equal to $24.6 \text{ mm}\cdot\text{yr}^{-1}$. The highest velocities values ($25 \text{ mm}\cdot\text{yr}^{-1}$ – $42 \text{ mm}\cdot\text{yr}^{-1}$) are recorded in the central part of the slope, while the lowest are measured near the NW and SW boundary of the landslide. Around the 60% of the persistent scatterers within the landslide have a velocity higher than $28 \text{ mm}\cdot\text{yr}^{-1}$, the 30% velocities less than $3 \text{ mm}\cdot\text{year}^{-1}$, and the 10% velocities between $3 \text{ mm}\cdot\text{yr}^{-1}$ and $28 \text{ mm}\cdot\text{yr}^{-1}$. Data from the field surveys, carried out several times since 2004, are consistent with the ground movements identified by the space-borne radar interferometry as the buildings and the roads are extensively interested by damages and cracks (Figure 3).

The displacement field and the velocities measured by the PSI technique match the boundary of the landslide and have confirmed the perimeter originally reported in the PAI. In particular it is worth noticing that the radar benchmarks located just outside NW portion of the landslide show velocity values of less than $1 \text{ mm}\cdot\text{yr}^{-1}$. These PS, difficult considering the error of the technique, can be considered as stable points. The analysis of the temporal evolution of the deformation during the time interval 1992–2001 has also included the analysis of the time series of displacement of each persistent

scatterers, samples of which are shown in Figure 6A,B. In particular the persistent scatterer AI697, located just inside Castagnola village, shows a total displacement in the acquisition period (1992–2001) of around 350 mm, while point AI735 shows a total displacement of around 260 mm.

Figure 6. Quantitative comparison among time series of two radar benchmarks ((A) AI735 and (B) AI697), inclinometers and crackmeters. The location of the instruments is reported in Figure 4.



A comparison between the PSI data, inclinometer readings and crackmeters, even though the two datasets were acquired during different periods (1992–2001 vs. 2001–2002), has shown a good agreement in terms of direction and deformation rates (Figure 5). In fact, taking into account of the acquisition geometry of the satellite for descending orbits, the radar measurements are compatible with the SW direction of movement recorded by the inclinometers.

As can be observed in Figure 4, quantitative comparison have been carried out for two groups of instruments, which are located enough close to be compared. In particular in Figure 6A it can be observed that the velocity of the radar benchmark AI735, computed taking into account the deformations measured from 1999 to 2001, is comparable with the mean annual velocity of the crackmeter F and inclinometer, 8 located nearby. In Figure 6B a good agreement can be observed, in terms of velocity, between crackmeter H and persistent scatterer AI697, while inclinometer 10 measures higher deformations and detects a phase of acceleration not inferable by the other instruments.

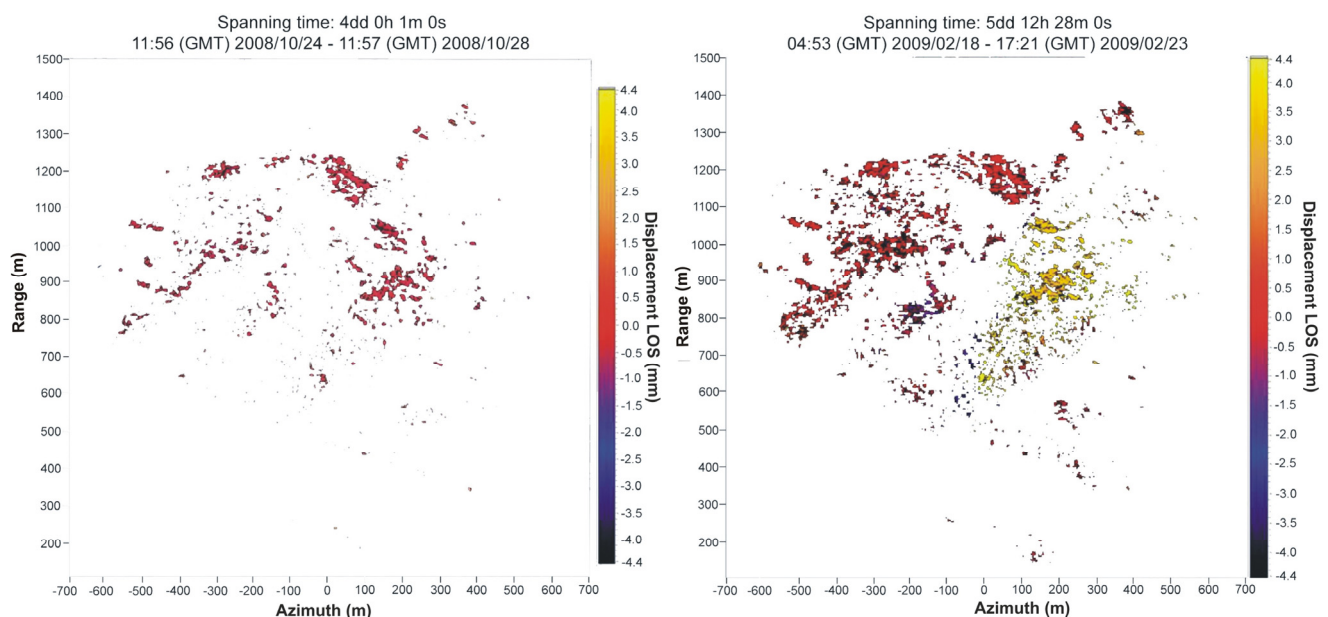
Concerning this, it is worth remembering that the PSI technique and the crackmeters measure deformations which are mainly the response of the buildings to surface ground movements. The inclinometers instead measure movements at depth, inside the landslide mass and the deformation at

the head of each instrument represents the cumulated displacement measured along each borehole. Furthermore, while inclinometers measure the horizontal component of the real movement vector, the PSI techniques evaluates only the line of sight (l.o.s.) component of the displacement. In particular, in the Castagnola village area, the PSI mean velocities vary from $15 \text{ mm}\cdot\text{yr}^{-1}$ to $42 \text{ mm}\cdot\text{yr}^{-1}$, while the mean velocities of inclinometers vary from $35 \text{ mm}\cdot\text{yr}^{-1}$ to $86 \text{ mm}\cdot\text{yr}^{-1}$. Moving downslope, there is a general decrease of velocity recorded both by the PSI and inclinometers.

4.2. GB-InSAR

Concerning the GB-InSAR, the analysis of the interferograms sequence related to the October 2008 campaign did not show any significant slope movements (Figure 7). The total displacements recorded during the second (February 2009) and third (February–March 2009) campaigns are represented by the cumulated displacements map of Figure 8. At the same time, a total of nine significant points (P_01 to P_09, in Figure 9) distributed over the slope were analyzed in order to determine velocity trends in key sectors of the landslide.

Figure 7. Interferograms elaborated from the data acquired during the first two campaigns. On the left, interferogram spanning a time interval of four days (between 24 and 28 October 2008); on the right, interferogram relative to the second campaign spanning a time interval of five days (between 18 and 23 February 2009).



The displacement map analysis highlights a large sector affected by movements that extends, approximately between 500 and 1,300 m, away from the radar sensor and corresponds to the SE sector of the landslide. The cumulative displacement map shows a maximum displacement rate of about $60 \text{ mm}\cdot\text{month}^{-1}$ in the head scarp area, near the Rovereto abandoned village and on the left side of the Rovereto creek valley (Tari area). The area where Castagnola village is located, is, instead, characterized by a lower deformation rate, equal to $20\text{--}25 \text{ mm}\cdot\text{month}^{-1}$. In the NW landslide sectors, ground deformation decreases dramatically, reaching a value of $4\text{--}5 \text{ mm}\cdot\text{month}^{-1}$ in the vicinity of Passano, Posata, Lazzino, Narà, and Voltorara villages. The landslide toe (SW landslide sector close to

Castagnola creek) was not covered by the radar signal and therefore the displacement information is missing. The time series analysis concerning some points of interest extracted from the interferograms (Figure 9) denotes that the displacement rate has decreased during the radar survey: maximum velocity was between $0.06\text{--}0.1\text{ mm}\cdot\text{h}^{-1}$ during the first week changing to $0.03\text{--}0.06\text{ mm}\cdot\text{h}^{-1}$ since the end of the second campaign (17–18 February 2009). In the second and third monitoring week (third campaign) the deformation rate remained nearly constant although it has been possible to recognize slightly velocity increases. The overall decrease of the velocity also corresponds to a decrease in the surface area affected by deformations. In the N monitored area (see point P_01, P_02, and P_03 in Figure 9), the overall velocity is close to zero and the area can be considered stable.

Figure 8. Cumulated displacement map of the Castagnola landslide obtained from the second and third campaigns (11 February 2009–13 March 2009).

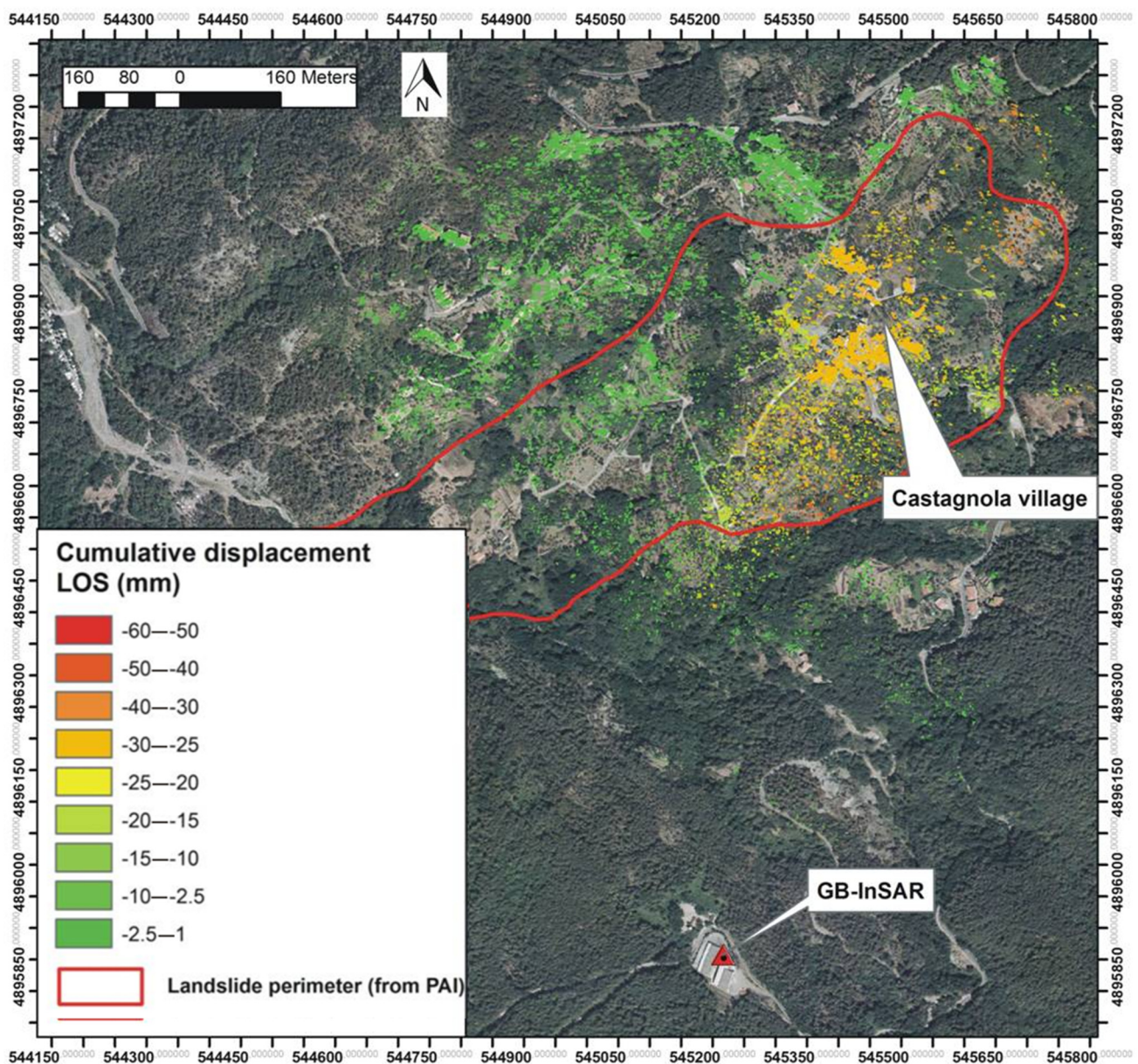
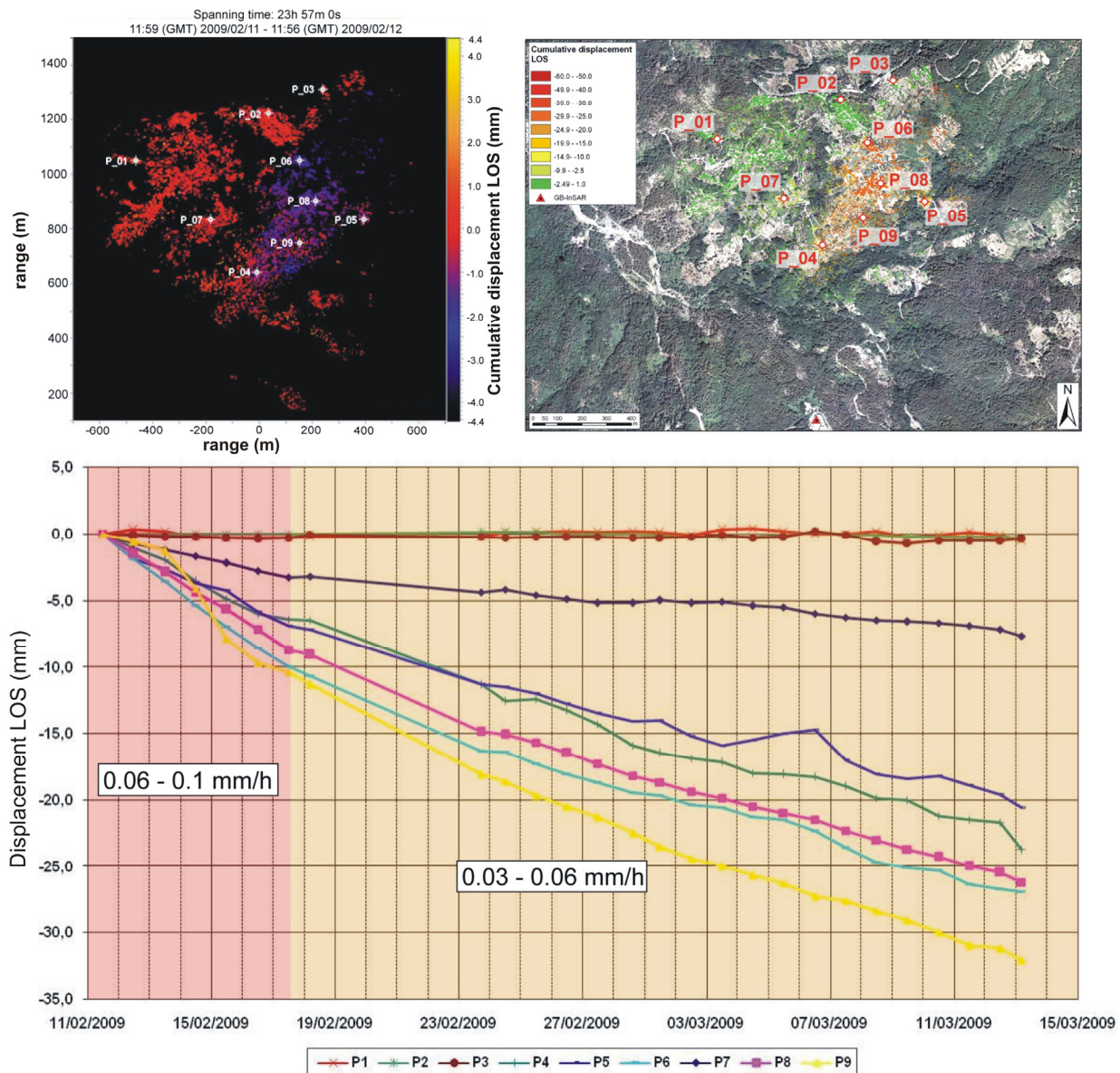


Figure 9. Time series analysis of nine points of the monitored area. The location of the points is shown both on the interferogram (upper left corner) and on the landslide map (upper right corner).



5. Discussion

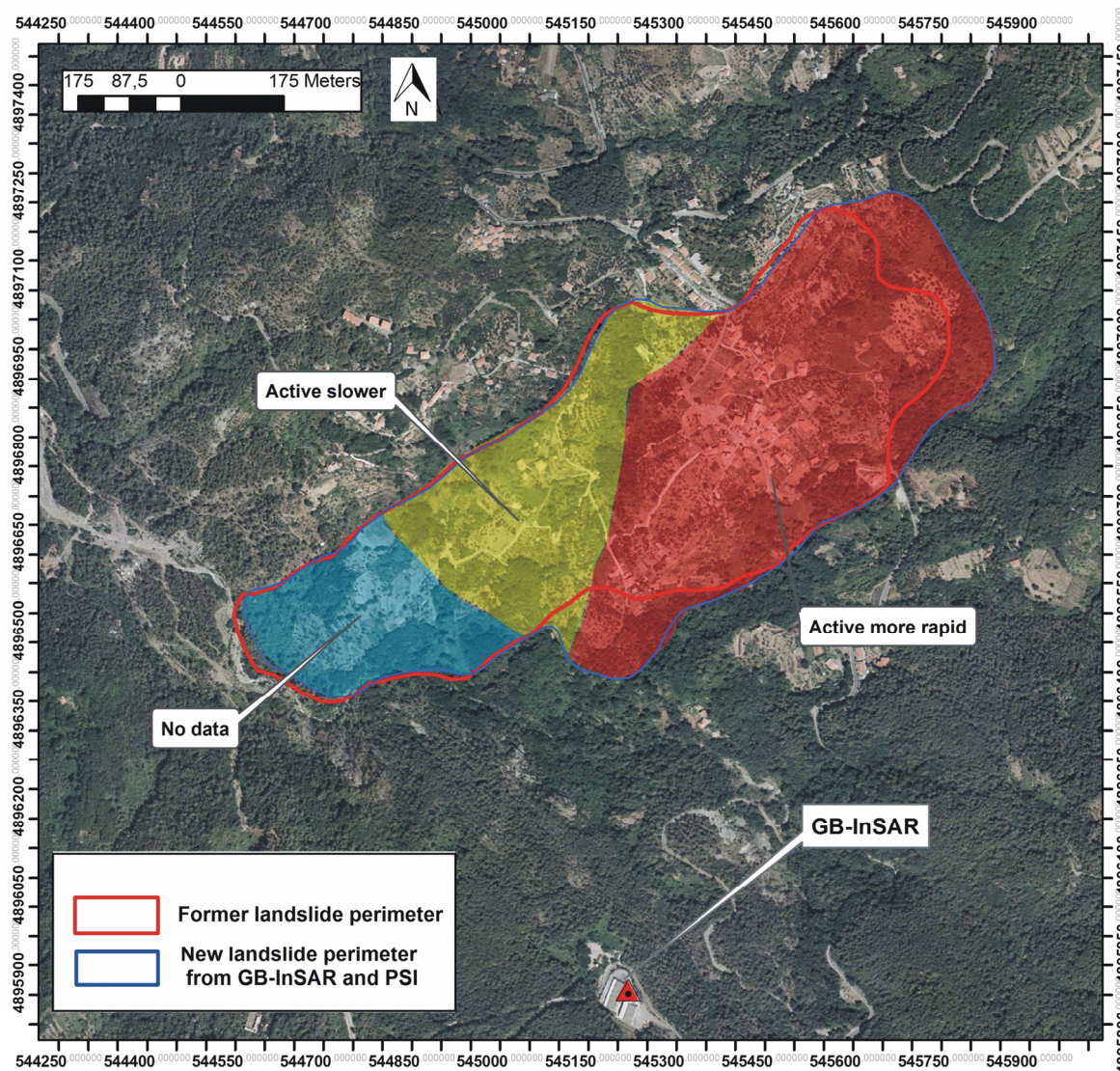
The analysis of the Castagnola landslide, by means of the remote sensing data has allowed to update its boundaries and to quantify the mean velocity of movements.

The interpretation of the outcomes of GBInSAR data has allowed deriving a multi-temporal deformation map of the landslide, showing the up-to-date displacement field and the mean landslide velocity.

In particular, the results of the GBInSAR second and third surveys have shown that the E and the SE landslide sectors during February and March 2009, have been characterized by maximum deformation rates, one order of magnitude higher (up to $50 \text{ mm} \cdot \text{month}^{-1}$) than the mean deformation rates recorded with the PSI technique in the period 1992–2001. The spatial distribution of

displacements detected by the two techniques is similar, with a huge sector affected by major movements extending approximately on the SE portion of the slope and correspond to Castagnola village.

Figure 10. Updated landslide perimeter and landslide intensity zonation.



Based on the GB-InSAR results, the boundaries of the Castagnola landslide have been updated and extended (Figure 10) towards the NE (main scarp area) and towards the S (Rovereto-Pallareto area). Moreover, it has been possible to differentiate an E sector (red in Figure 10) characterized by an average rate of deformation of about $0.055 \text{ mm} \cdot \text{h}^{-1}$ and a W sector (yellow in Figure 10) characterized by a lower average deformation rate ($0.025 \text{ mm} \cdot \text{h}^{-1}$). With regard to the landslide toe (light blue area in Figure 10) any consideration about the velocity cannot be drawn since the area was not covered by the radar signal.

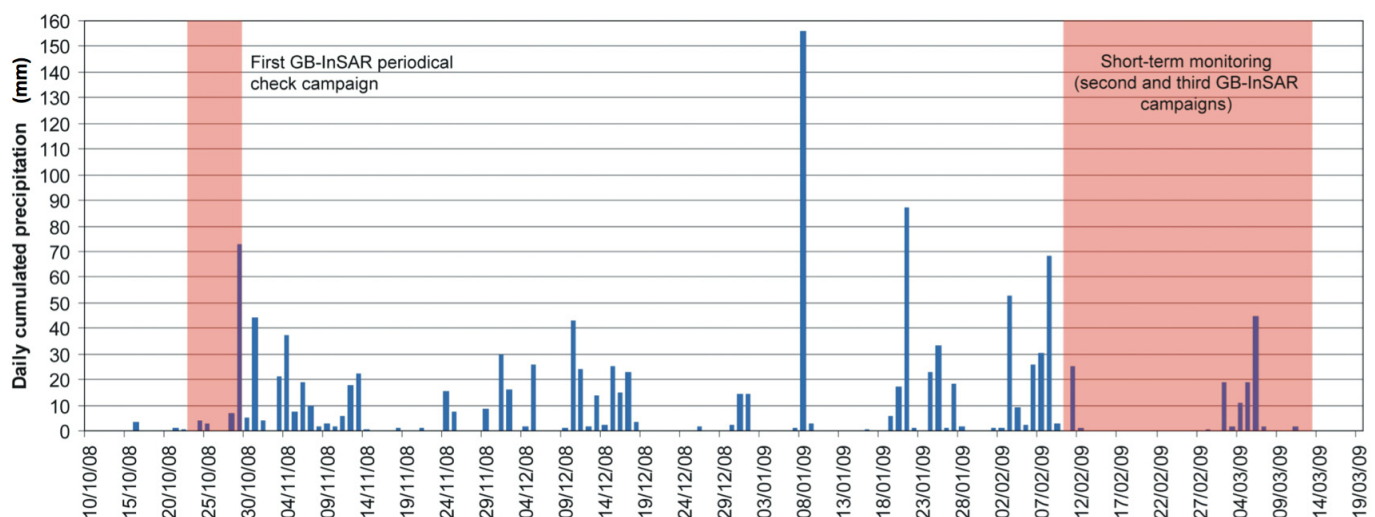
The difference between PSI and GBInSAR deformation rates has to be ascribed both to the different acquisition period (1992–2001 vs. 2009) and to the intrinsic difference of the techniques. The PS analysis is carried out only on stable scatterers distributed over the landslide surface in which phase response is enough coherent over time. Due to the temporal baseline of the space-borne radar sensor (35 days for ERS1–ERS2), areas characterized by rapid geometric changes are discarded from the

analysis due to the loss of the short-term coherence. In such a case, the landslide sectors characterized by rapid deformations are not likely included in the PSI analysis.

The GBInSAR results highlight that the Castagnola landslide during February 2009, has undergone a pronounced acceleration phase. The triggering mechanism of the landslide acceleration phases can be surely related to rainfall events. In Figure 11, the daily-cumulated precipitation recorded, from October 2008 to March 2009, by a rain gauge located on the vicinity of Castagnola village is shown. The graph highlights that November and the first 20 days of December 2008, have been characterized by prolonged rainfall events, followed by a less rainy period, except for the major event of 8 January 2009 (156 mm). It is worth noting that the landslide acceleration phase has been recorded by the GBInSAR monitoring at the end of a further prolonged period of heavy rainfall (25 days) started on 20 January 2009. The decrease of the deformation rate recorded during the third campaign, occurred only one week after the end of the rainy period previously described. A further slight and short acceleration phase was recorded just after the rainfall event (98.5 mm cumulated) occurred in the first few days of March 2009.

Hence, it is clear that the most important triggering mechanism of landslide is the pore pressure build-up inside the slope and the correspondent decrease of the effective stress along sliding surfaces. Moreover, the poor mechanical properties of the Palombini Shales due to the pervasive weathering and the regional tectonic stresses that dismantled their structure, as well as the continuous erosion at the landslide toe and deepening of the Castagnola and Rovereto creek, contribute to maintain unfavorable slope equilibrium conditions.

Figure 11. Daily cumulated precipitation recorded from October 2008 to March 2009, in the Castagnola area.



6. Conclusions

The paper has reported the application of both satellite and ground-based radar interferometry, integrated to conventional monitoring systems, for the zonation of the intensity related to the Castagnola landslide.

The analysis of the instability conditions of the Castagnola landslide started in 2001 when 10 inclinometers and 10 crackmeters were installed. The outcomes of the monitoring campaign, started

in April 2001, and finished in April 2002, has allowed to detect the depth of the sliding surface and to define the deformation rates. In order to investigate the past-long term evolution of the ground movements a PSI (Persistent Scatterers Interferometry) analysis has been performed making use of set of ERS1/ERS2 images, acquired in 1992–2001 period. This technique has allowed to confirm the landslide boundaries as mapped in the PAI (Hydrogeological Setting Plan) and to define the landslide intensity in terms of velocity. A qualitative comparison of PSI results and inclinometric measurements has been performed, showing a good agreement between the two techniques in terms of direction and deformation rates of the movement.

The results of the monitoring campaign by means of ground-based radar interferometry (GBInSAR) carried out discontinuously from October 2008 to March 2009, has shown deformation rates, higher with respect to the PSI technique. On the basis of the outcomes of GBInSAR monitoring, the boundaries of the Castagnola landslide have been updated and a zonation of the landslide into sectors with different degree of intensity has been performed. Furthermore the GBInSAR technique has highlighted the link between the acceleration of the phenomena and the triggering factor. In particular, it has been observed how the increase in the rainfall intensity causes an increase of the deformation rates.

Two landslide sectors, characterized by different displacement rates, have been identified and the area affected by movements has been extended. Hence, the new landslide intensity zonation obtained could be directly exploited as a new tool for appropriate planning and development.

This type of analysis gives information on spatial and temporal deformation pattern and is fundamental for evaluating the possible landslide evolution, defining deformation thresholds, and setting real-time monitoring systems for early warning purpose.

Furthermore, the combination of PSI and GB-InSAR has demonstrated as an efficient tool to retrieve past and real-time displacement data, which can support the definition of appropriate risk management strategies. This tool can be a sound base to develop new techniques for mapping and monitoring, not only landslides, but also other types of natural hazards.

Acknowledgments

The work described in this paper was performed in the framework of two consulting contracts “Monitoraggio dei fenomeni franosi in località Castagnola (La Spezia) mediante interferometria con sensori basati a terra” and “Monitoraggio dei fenomeni franosi in località Castagnola (La Spezia) mediante interferometria SAR satellitare” between Earth Sciences Department of Università degli Studi di Firenze (DST-UNIFI) and Provincia di La Spezia. The authors would like to acknowledge Provincia di La Spezia for providing the *in situ* monitoring data and in particular Marco Del Soldato. Ellegi LiSALab and Tele-Rilevamento Europa are also acknowledged for providing the GBInSAR systems used for data acquisition and their processing and for the data processing of the PSInSAR data respectively. Francesco Antolini and Guido Luzi are acknowledged for their support during landslide and the GBInSAR campaign survey. The authors would like to acknowledge three anonymous referees for the helpful and valuable revisions.

Author Contributions

Veronica Tofani has contributed to the geological and geomorphological survey and to the realization of the landslide model. She has interpreted the PSI data and elaborated the inclinometers data. She has written the paper.

Chiara Del Ventisette has contributed to the geological and geomorphological survey, to the realization of the landslide model. She has elaborated and interpreted the GB-InSAR data.

Sandro Moretti and Nicola Casagli have supervised and coordinated the research activity and have provided their suggestions and revisions during the writing of the paper.

Conflicts of Interest

The authors declare no conflicts of interest.

References

1. Hungr, O. *Some Methods of Landslide Hazard Intensity Mapping*; Cruden, D., Fell, R., Eds.; Landslide Risk Assessment, Balkema: Rotterdam, The Netherlands, 1997.
2. IUGS Working Group on Landslides. A suggested method for describing the rate of movement of a landslide. *Bull. Int. Assoc. Eng. Geol.* **1995**, *52*, 75–78.
3. Cruden, D.M.; Varnes, D.J. Landslide Types and Processes. In *Landslides-Investigation and Mitigation*; Turner, A.K., Schuster, R.L., Eds.; Transportation Research Board: Washington, DC, USA, 1996; Chapter 3; pp. 36–75.
4. Fell, R.; Corominas, J.; Bonnard, C.; Cascini, L.; Leroi, E.; Savage, W.Z.; On behalf of the JTC-1 Joint Technical Committee on Landslides and Engineered Slopes. Guidelines for landslide susceptibility, hazard and risk zoning for land use planning. *Eng. Geol.* **2008**, *102*, 85–98.
5. Colesanti, C.; Ferretti, A.; Prati, C.; Rocca, F. Monitoring landslides and tectonic motions with the permanent scatterers technique. *Eng. Geol.* **2003**, *68*, 3–14.
6. Canuti, P.; Casagli, N.; Ermini, L.; Fanti, R.; Farina, P. Landslide activity as a geoindicator in Italy: Significance and new perspectives from remote sensing. *Environ. Geol.* **2004**, *45*, 907–919.
7. Ferretti, A.; Prati, C.; Rocca, F. Permanent scatterers in SAR interferometry. *IEEE Trans. Geosci. Remote Sens.* **2001**, *39*, 8–20.
8. Lu, P.; Casagli, N.; Catani, F.; Tofani, V. Persistent Scatterers Interferometry Hotspot and Cluster Analysis (PSI-HCA) for detection of extremely slow-moving landslides. *Int. J. Remote Sens.* **2012**, *33*, 466–489.
9. Del Ventisette, C.; Ciampalini, A.; Calò, F.; Manunta, M.; Paglia, L.; Reichenbach, P.; Colombo, D.; Mora, O.; Strozzi, T.; Garcia, I.; *et al.* Exploitation of large archives of ERS and ENVISAT C-Band SAR data to characterize ground deformation. *Remote Sens.* **2013**, *5*, 3896–3917.
10. Tofani, V.; Segoni, S.; Agostini, A.; Catani, F.; Casagli, N. Technical note: Use of remote sensing for landslide studies in Europe. *Nat. Hazards Earth Syst. Sci.* **2013**, *13*, 299–309.
11. Tofani, V.; Raspini, F.; Catani, F.; Casagli, N. Persistent Scatterer Interferometry (PSI) technique for landslide characterization and monitoring. *Remote Sens.* **2013**, *5*, 1045–1065.

12. Crosetto, M.; Monserrat, O.; Jungner, A.; Crippa, B. Persistent Scatterers Interferometry: Potential and Limits. Available online: http://www.isprs.org/proceedings/XXXVIII-1-4-7_W5/paper/papers.htm (accessed on 9 January 2013).
13. Righini, G.; Pancioli, V.; Casagli, N. Updating landslide inventory maps using Persistent Scatterer Interferometry (PSI). *Int. J. Remote Sens.* **2012**, *33*, 2068–2096.
14. Tarchi, D.; Casagli, N.; Fanti, R.; Leva, D.; Luzi, G.; Pasuto, A.; Pieraccini, M.; Silvano, S. Landslide monitoring by using ground-based SAR interferometry: An example of application to the Tessina landslide in Italy. *Eng. Geol.* **2003**, *68*, 15–30.
15. Del Ventisette, C.; Intrieri, E.; Luzi, G.; Casagli, N.; Fanti, R.; Leva, D. Using ground based radar interferometry during emergency: The case of the A3 motorway (Calabria Region, Italy) threatened by a landslide. *Nat. Hazard. Earth Syst. Sci.* **2011**, *11*, 1–13.
16. Del Ventisette, C.; Casagli, N.; Fortuny-Guasch, J.; Tarchi, D. Ruinon landslide (Valfurva, Italy) activity in relation to rainfall by means of GBInSAR monitoring. *Landslides* **2012**, *9*, 497–509.
17. Pieraccini, M.; Casagli, N.; Luzi, G.; Tarchi, D.; Mecatti, D.; Noferini, L.; Atzeni, C. Landslide monitoring by ground-based radar interferometry: A field test in Valdarno (Italy). *Int. J. Remote Sens.* **2003**, *24*, 1385–1391.
18. Gischig, V.; Loew, S.; Kos, A.; Moore, J.R.; Raetzo, H.; Lemy, F. Identification of active release planes using ground-based differential InSAR at the Randa rock slope instability, Switzerland. *Nat. Hazards Earth Syst. Sci.* **2009**, *9*, 2027–2038.
19. Herrera, G.; Fernández-Merodo, J.A.; Mulas, J.; Pastor, M.; Luzi, G.; Monserrat, O. A landslide forecasting model using ground based SAR data: The Portalet case study. *Eng. Geol.* **2009**, *105*, 220–230.
20. Barla, G.; Antolini, F.; Barla, M.; Mensi, E.; Piovano, G. Monitoring of the Beauregard landslide (Aosta valley, Italy) using advanced and conventional techniques. *Eng. Geol.* **2010**, *116*, 218–235.
21. Abbate, E.; Bortolotti, V.; Principi, G. Apennine ophiolites: A peculiar oceanic crust. *Ophioliti* **1980**, *1*, 59–96.
22. Principi, G.; Bortolotti, V.; Chiari, M.; Cortesogno, L.; Gaggero, L.; Marcucci, M.; Saccani, E.; Treves, B. The pre-orogenic volcano-sedimentary covers of the Western Tethys oceanic basin: A review. *Ophioliti* **2004**, *29*, 177–211.
23. Rudolf, H.; Leva, D.; Tarchi, D.; Sieber, A.J. A Mobile and Versatile SAR System. In Proceedings of the IEEE 1999 International Geoscience and Remote Sensing Symposium, Hamburg, Germany, 28 June–2 July 1999; pp. 592–594.